



REGULAR ARTICLE

Study of the Elemental Composition of Thin Nanocrystalline Films of CoNi and FeNi Alloys by X-ray Spectral Microanalysis

V.B. Loboda* , S.M. Khursenko, V.O. Kravchenko, V.M. Zubko, A.V. Chepizhnyi

Sumy National Agrarian University, 40021 Sumy, Ukraine

(Received 12 January 2025; revised manuscript received 22 April 2025; published online 28 April 2025)

The article presents the results of studying the elemental composition of CoNi and FeNi alloy nanocrystalline films by X-ray spectral microanalysis (X-ray microanalyzer based on an energy-dispersive spectrometer, which is part of the REM-103-01 scanning electron microscope). The alloy films with thicknesses of 10-200 nm were obtained by condensation of evaporated initial massive binary CoNi and FeNi alloys in a vacuum of 10^{-4} Pa. The CoNi alloys were evaporated by an electron beam using an electron diode gun with a condensation rate of 0.5-1.5 nm/s. The purity of the initial Co and Ni metals was at least 99.9 %. The concentrations of the CoNi alloy film components varied over a wide range. The FeNi alloy films were obtained by evaporation of Permalloy 50N technical alloy. The characteristic X-ray spectrum of the film substance was excited by scanning a film section with dimensions of $300 \times 300 \mu\text{m}$ with an electron beam; for thicker films, the scanning section size was $1 \times 1 \mu\text{m}$. Thin Ni films of the same thickness were used as standards when conducting quantitative measurements of the elemental composition of alloy films of a certain thickness. The results of X-ray microanalysis indicate high purity of the films. Comparison of the results of X-ray microanalysis measurements of the concentrations of the initial alloys and the obtained films showed their coincidence within the limits of the analysis error.

Keywords: X-ray spectral microanalysis, Chemical composition, Thin films, Nanocrystalline films, Alloys.

DOI: [10.21272/jnep.17\(2\).02020](https://doi.org/10.21272/jnep.17(2).02020)

PACS numbers: 81.15. – z, 82.80.Ej

1. INTRODUCTION

The study of the physical properties of thin metal films is due both to the possibility of obtaining results that would contribute to solving a number of fundamental problems of solid-state physics, and to the prospects for their practical application. In recent years, considerable attention has been paid to the study of thin magnetic films, which is caused by a number of their unique properties, in particular, the discovery of the phenomenon of giant magnetoresistance in spatially modulated systems and multilayer film structures, and its application for the development of magnetic read heads, magnetic sensors, and magnetoresistive memory.

Along with the creation of pure metal films, a promising direction is the production of magnetic alloy films [1-3] and multilayer systems based on binary alloys of ferromagnetic metals (Co, Fe, Ni) [4-5]. The advantage of alloys over pure metals is that by changing their composition, materials with improved physicochemical, mechanical and operational properties can be obtained. However, the problem of developing a technology for producing film alloys of a given composition, structure and with the necessary properties remains relevant. Along with traditional film directions, in recent decades a scientific direction has been formed associated with improving the service properties of massive metal samples by methods of creating layered structures in modified surface layers [6-7].

The physical properties of thin metal films, both in scientific and practical terms, are of considerable interest to researchers. Films of magnetically ordered metals (Ni, Co, Fe and their alloys) occupy a special place in the physics of thin films. This is due to the discovery in recent years of a number of new fundamental effects in film objects based on them (giant magnetoresistance, spin-polarized tunneling, colossal magnetoresistance, etc.), which create the basis for the development of miniature magnetoelectronic devices, new methods of recording and storing information, new types of highly sensitive sensors, etc. This paper presents the results of a study of the elemental and chemical composition of CoNi and FeNi alloy films in a wide range of component concentrations.

2. EXPERIMENTAL METHODOLOGY AND TECHNIQUE

2.1 Preparation of Samples of Alloy Films

It is known [8] that two main groups of methods are used to obtain thin films of alloys: 1) formation of multi-component films directly on a substrate (separate evaporation of components; annealing of multilayer structures with diffusion mixing); 2) use of massive alloys of a predetermined composition (evaporation of finite weighed samples; explosive evaporation; evaporation under stationary conditions).

* Correspondence e-mail: loboda-v@i.ua



The second group of methods is quite promising from the point of view of practical application due to its relative simplicity. However, the properties of the films may change due to fractionation during evaporation and changes in the chemical and phase composition of the obtained film alloy compared to the original.

According to the phase diagram data (Fig. 1, [9]), for CoNi alloys at temperatures close to the melting point and in the liquid state in the entire concentration range, complete mutual solubility of the components is observed. In this case, the liquidus and solidus lines coincide, which eliminates the possibility of alloy fractionation during melting.

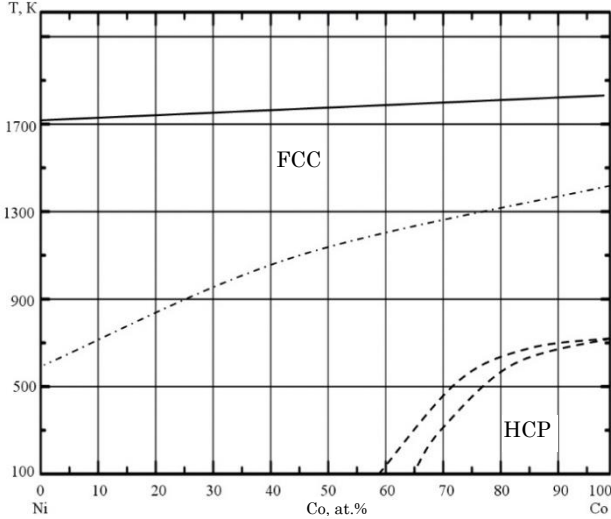


Fig. 1 – Phase diagram of CoNi alloy in bulk state [9]

In the general case, when evaporating binary alloys, the composition of the deposited film differs from the composition of the starting material due to the fact that one of the components may have a higher evaporation rate. The evaporation rate of the material at temperature T is determined by the well-known formula:

$$v = kp\sqrt{\frac{M}{T}} = A_1p, \quad (2.1)$$

where k is a constant; p is the vapor pressure; M is the molecular weight of the substance; T is the evaporation temperature.

When evaporating alloys in a vacuum, the vapor pressure of each component above the melt is determined by the alloy composition and differs from the values for the pure components. In the simplest case, the vapor pressure of component A in the presence of component B is determined by Raoult's law [10]:

$$\frac{p_A - p_{AB}}{p_A} = C_B, \quad (2.2)$$

where C_B is the atomic fraction of component B .

Let's obtain formulas for calculating the fractionation of binary systems during the evaporation of finite amounts. Let the evaporator initially contain a binary alloy with the mass content of components m_{01} and m_{02} . During the time dt , taking into account the expression for the evaporation rate (2.1), the decrease in the mass of each component is:

$$dm_A = -kp_{0A}f_A\sqrt{\frac{\mu_A}{T}}C_A(t)dt, \quad (2.3)$$

$$dm_B = -kp_{0B}f_B\sqrt{\frac{\mu_B}{T}}C_B(t)dt, \quad (2.4)$$

where k is a constant that depends on the choice of the system of units; p_{0A} , p_{0B} are the saturated vapor pressure of pure components A and B of the alloy at temperature T ; f_A , f_B are the activity coefficients of the components:

$$f_A = \frac{\alpha_A}{C_A}, \quad (2.5)$$

where $\alpha_A = \frac{p_{AB}}{p_A}$ is the activity of component A (similarly for component B); $C_A(t)$, $C_B(t)$ are the atomic fractions of components; μ_A , μ_B are their molar masses.

In the case of Raoult's law (ideal melts), we have:

$$1 - \frac{p_{AB}}{p_A} = C_B, \\ \alpha_A = \frac{p_{AB}}{p_A} = 1 - C_B = C_A, \quad (2.6)$$

whence $f_A = f_B = 1$.

According to [8], the same saturated vapor pressures for Co and Ni are achieved at similar temperatures (for example, $p_{Co} = 1.33$ Pa at $T = 1790$ K, p_{Ni} has the same value at $T = 1800$ K; a similar situation also occurs for higher pressure values), so it is possible to take $p_A = p_B$. In addition, the molar masses of Co and Ni are close ($\mu_{Co} = 58.9$ g/mol, $\mu_{Ni} = 58.7$ g/mol [11]), and, therefore, for the mass fractions of Co and Ni we obtain the ratio:

$$C_{Co} = \frac{C_{Co}\mu_{Co}}{C_{Co}(\mu_{Co} - \mu_{Ni}) + \mu_{Ni}} = \frac{58.9}{C_{Co}(58.9 - 58.7) + 58.7}C_{Co} = \\ \frac{58.9}{58.7 + 0.2C_{Co}}C_{Co} \approx C_{Co}. \quad (2.7)$$

Thus, under the condition of fulfilling Raoult's law, the concentration of components in the CoNi film alloy should be the same as in the bulk sample, and the films should be homogeneous in chemical composition.

Taking into account these considerations, to obtain CoNi film samples, we chose the method of evaporation of alloys of a predetermined composition.

The starting material for CoNi alloy films was prepared as massive samples of the corresponding composition. Pure metals (not worse than 99.9 %) were used to prepare the samples. The concentration of components was changed by changing the mass ratios of metals (the relative error of mass determination did not exceed 5 %). The samples were prepared by melting the starting materials in a ceramic crucible under high vacuum conditions with a holding time of 1 h at a temperature close to melting temperature T_s for homogenization. The mass loss did not exceed 1-2 %.

The starting material for the FeNi alloy films was the Permalloy 50N technical alloy.

Alloy films with a thickness of 10-200 nm were obtained in high vacuum 10^{-4} Pa by electron beam evaporation of prepared alloys and Permalloy 50N using a diode-type electron gun. Film deposition was carried out on substrates at room temperature 300 K. The condensation rate, which was determined by the deposition time and sample thickness, was maintained approximately constant during the

condensation process and was 0.5-1.5 nm/s depending on the evaporation mode. Condensation of film samples was carried out without applying an orienting magnetic field (excluding the Earth's magnetic field).

The design of the substrate holder (Fig. 2) allowed to obtain four film samples (2, Fig. 2) of the same composition with different thicknesses in one technological cycle of sputtering. The geometric dimensions of the samples were set by special masks made with high precision from nichrome foil with holes of the desired shape and size.

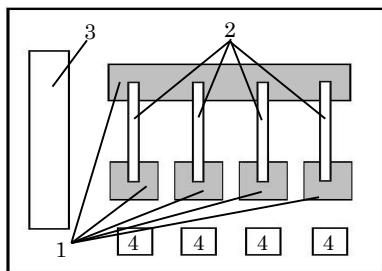


Fig. 2 – The scheme of the substrate holder: 1 – contact pads; 2 – film samples; 3 – «witness» glass; 4 – KBr single crystals with carbon films

To study the chemical and elemental composition, as well as the electrical conductivity and magnetoresistance, the samples were deposited on polished optical glass substrates. Copper contact pads (1, Fig. 2) with a chromium underlayer were previously applied to these substrates to improve adhesion to the glass. For structural studies, KBr single crystals with carbon films (4) were used as substrates. In addition, glass «witness» plates (3) were fixed on the substrate holder to measure the thickness. The substrates were treated according to the standard procedure described in [8], which included chemical cleaning followed by boiling in distilled water and drying, as well as degassing by heating to 600 K for 30 min in a vacuum chamber.

The thickness of the films was measured using a microinterferometer MII-4 with a laser light source (miniature semiconductor laser, $\lambda = 647$ nm). The interference pattern was recorded using a digital camera with data transmission to a computer. With this method of measurements, it is possible to reduce the error in measuring the thickness, especially in the range of thicknesses $d < 50$ nm. An additional reduction in the error can be achieved by determining the thickness using glass plates «witnesses», on which, according to the geometric conditions of deposition (Fig. 3), the film of the greatest thickness was condensed.

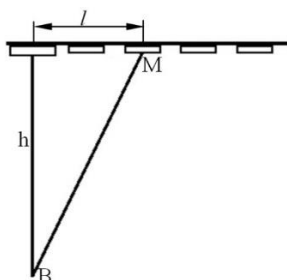


Fig. 3 – Geometry of the «substrate-evaporators» system for calculating film thickness

In this case, a calculation method was also used to determine the thickness of the films. The thickness of the film deposited at point M (Fig. 3), in the case of evaporator B with a small surface area, can be calculated by the relationship [8]:

$$d = d_0 \left[1 + \left(\frac{l}{h} \right)^2 \right]^{-2}, \quad (2.8)$$

where d_0 is the thickness of the «witness» film at a point above the evaporator; l is the distance from the middle of the «witness» to point M ; h is the distance from the evaporator plane to the substrate plane.

The measurement error is 5-10 % for thicknesses 50-200 nm and 10-15 % for thickness $d < 50$ nm. For ultrathin ($d < 15$ nm) films, we also used a comparison of data from interferometric measurements and microphotometric studies based on an extrapolated calibration curve constructed from data for thicker films. In this case, the film thickness d is usually understood as the weighted film thickness, since in this case we can only talk about the effective (reduced) film thickness.

2.2 Method for Studying the Elemental Composition of Film Samples by X-ray Microanalysis

To verify the assumption of the correspondence of the composition of the initial bulk alloy and the resulting film alloy, a study of the elemental composition of the initial alloy samples and thin films of CoNi alloys was carried out using an X-ray microanalyzer installed on a REM-103-01 scanning electron microscope, as in the work [12]. This method is based on determining the intensities and wavelengths of characteristic X-ray lines excited as a result of bombardment of the sample with fast electrons with energies up to 100 keV [13]. In this case, an energy-dispersive spectrometer (EDS) was used to analyze the chemical composition of the sample, the scheme of which is presented in Fig. 4.

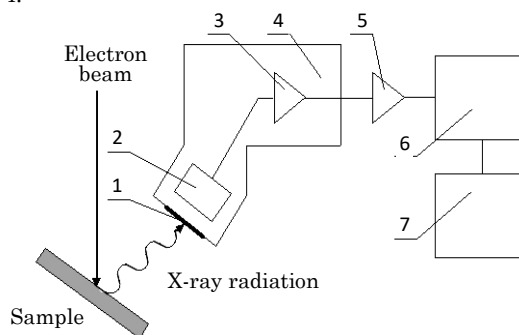


Fig. 4 – Scheme of the spectrometer with EDS

The characteristic X-ray radiation generated in the sample as a result of its interaction with an electron beam with an energy of 20-100 keV is directed through a beryllium window (1) into a cryostat (4) onto a solid-state semiconductor detector (2) made of lithium-doped silicon. To reduce the detector's intrinsic noise, it is cooled in the cryostat to a liquid nitrogen temperature of $T = 77$ K. In the detector, photoelectrons with different energies are generated under the action of absorbed X-ray quanta. The photoelectrons spend most of their energy on the formation of electron-hole pairs, which, in turn, are separated by an

plied voltage and form a charge pulse, which creates a voltage pulse in the preamplifier (3). The weak signal after the preamplifier is amplified and finally formed by a final amplifier (5) and enters a multi-channel analyzer (6), where the pulses are separated depending on their amplitude. The processing of the separated pulses is carried out using computer software (7) and is displayed on the monitor screen in the form of a spectrum – the dependence of the number of pulses on the energy of X-ray quanta.

Since the amount of substance in film samples with a thickness of up to 100 nm is extremely small, to increase the intensity of the characteristic X-ray lines from such samples, we used scanning electron microscope beam of a film section with a size of $300 \times 300 \mu\text{m}^2$. This made it possible to obtain, to some extent, integrated data on the chemical composition of the film without overheating it (without introducing radiation damage). For massive samples and thick films ($d > 100 \text{ nm}$), the size of the electron probe was reduced to $1 \mu\text{m}^2$.

The accuracy of X-ray microanalysis of the elemental composition of a substance is determined by a number of factors (electron probe beam current, accelerating voltage (electron energy), choice of standard, etc.), as a result of which there is a need to introduce corrections that take into account differences in electron scattering, X-ray generation and X-ray emission for the sample and standard. Most of the existing correction methods (the method of «matrix» corrections or ZAF corrections, the empirical method, etc.) can be applied only to the analysis of the composition of bulk samples. Although the theoretical foundations of the study of the quantitative composition of a film sample by X-ray spectral analysis are based on the same model concepts of the interaction of electrons with matter as for bulk samples, for films a number of features should be taken into account, associated with the difference in the processes of formation, absorption and transmission of X-ray radiation in samples of limited thickness.

One of the methods used in the analysis of the chemical composition of thin films is based on comparing the radiation intensities of a certain element in the sample and a massive standard of this element [13]. To determine the mass concentration of C_A , the following relationship is used:

$$\frac{I}{I_0} = \frac{QS}{C_{AR}} Dd, \quad (2.9)$$

where I and I_0 are the intensities of the characteristic lines for the sample and standard, respectively; R is the backscattering factor, which takes into account the decrease in intensity due to the escape of part of the electrons from the target due to the small thickness of the sample; S is the braking factor, which takes into account the energy losses of electrons during their interaction with the target atoms; Q is the ionization cross section of the atoms of the substance; D is the density of the sample; d is the thickness of the sample.

It is obvious that the estimation of the mass thickness Dd of a film sample is a source of significant errors, as a result of which the use of massive standards in X-ray spectral analysis of films is limited.

More effective is the method using a thin film of known composition (in particular, a film of a pure element) as a standard. Then the ratio of the intensities of the sample and the standard can be written as:

$$\frac{I}{I_{st}} = \frac{C_A D d}{C_{st} D_{st} d_{st}}, \quad (2.10)$$

In the case of close values of the density of the components of the ratio from (2.10) we obtain:

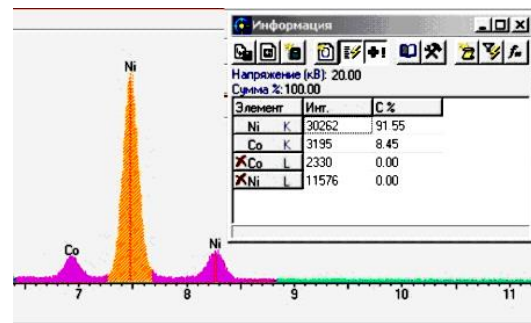
$$C_A = C_{st} \frac{I d_{st}}{I_{st} d}. \quad (2.11)$$

When conducting quantitative analysis of CoNi and FeNi alloy films, thin films of pure Ni ($C_{st} = 1$) were used as a reference, which made it possible to calculate the nickel concentration in the samples using the relationship (2.11). Considering that the alloy films are binary, the concentration of the second component can be found as $C_B = 1 - C_A$.

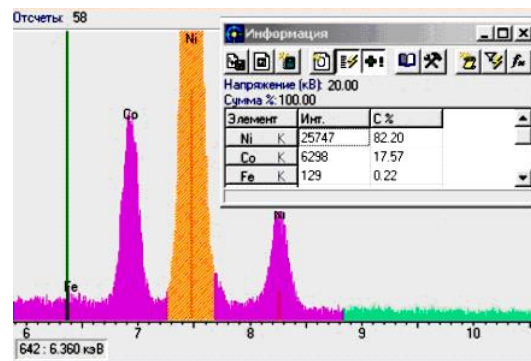
3. RESULTS AND DISCUSSION

3.1 CoNi Alloy Films

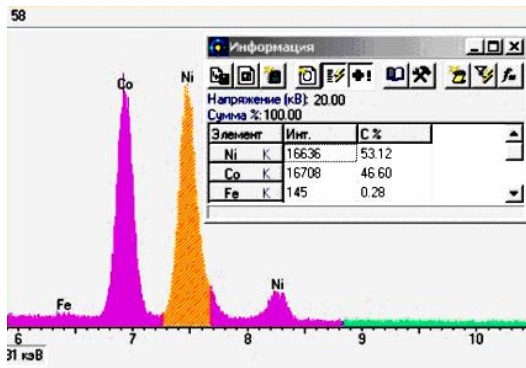
To obtain the films, the method of evaporation of finite weighed samples was used. For evaporation, we produced a series of massive CoNi alloys of known composition. To verify the considerations regarding the correspondence of the composition of CoNi film alloys to the composition of the samples, we conducted studies of the composition of the samples and films by the method of X-ray microanalysis using an X-ray microanalyzer with analysis of the energy of X-ray photons using EDS. Fig. 5 shows the energy spectra of characteristic X-ray radiation for massive samples of CoNi alloy of different composition. The results of microanalysis are summarized in Table 1. As can be seen from the results of computer processing of these spectra (using the microanalyzer software), the composition of the prepared alloys (samples) within the measurement error corresponds to their calculated composition during their preparation.



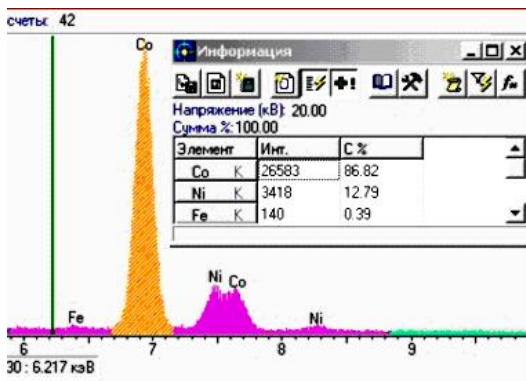
a



b



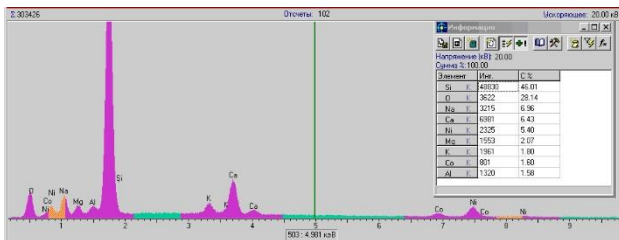
c



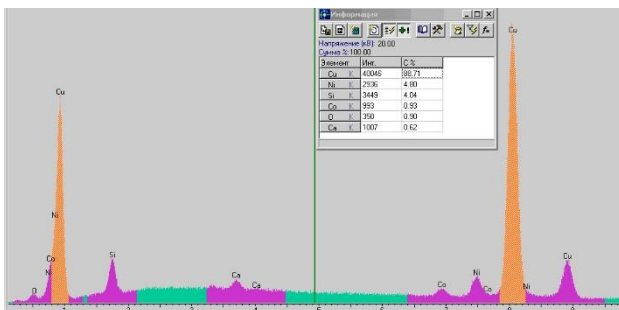
d

Fig. 5 – Characteristic X-ray spectra of the initial batches of the CoNi alloy (Co content, wt. %: a – 10 %; b – 20 %; c – 50 %; d – 90 %)

The energy spectra of the characteristic X-ray radiation of alloy films are presented in Fig. 6 and Fig. 7.

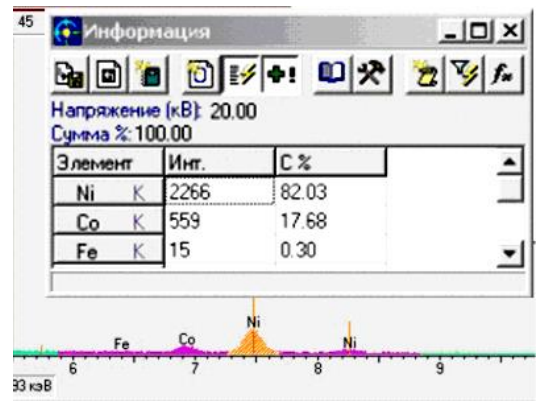


a

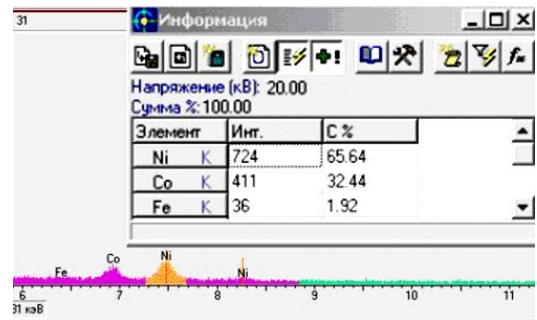


b

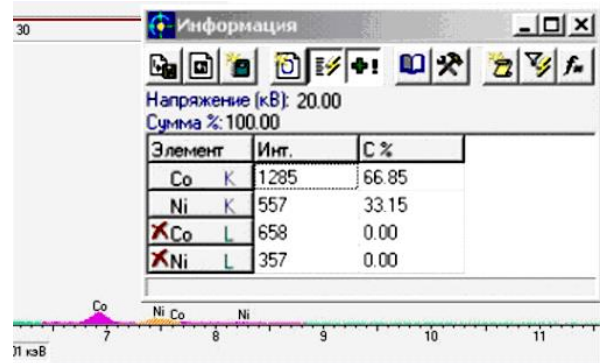
Fig. 6 – Characteristic X-ray spectra from a CoNi alloy film on a glass substrate (a) and on a copper contact pad (b)



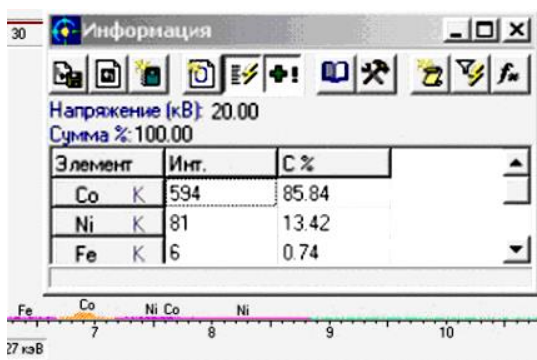
a



b



c



d

Fig. 7 – Characteristic X-ray spectra of CoNi film alloys (Co content, wt. %: a – 20 %; b – 40 %; c – 70 %; d – 90 %)

Analysis of characteristic X-ray spectra shows that in the region of the CoNi film on a glass substrate

(Fig. 6 a) there are only lines of the substrate material (left part of the spectrum) and the film material (right part of the spectrum). In the region of the overlap of the film and the contact pad, there are lines of both the film material and the contact pad and the substrate. No other impurities are observed according to the data of the micro-X-ray spectral analysis.

The energy spectra of the characteristic X-ray radiation of the alloy films (Fig. 7, Table 1) indicate that the assumption of the identity of the composition of the films and the composition of the bulk initial samples is generally confirmed.

Table 1 – Chemical composition of the initial samples of CoNi alloy and the corresponding CoNi film alloys according to X-ray spectral microanalysis

Calculated content of elements in samples, wt.%		Content of elements in samples according to microanalysis results, wt.%		Element content in the film alloy, wt.%			
Co	Ni	Co	Ni	Calculation using the program (taking into account corrections)		Calculation without taking into account corrections	
Co	Ni	Co	Ni	Co	Ni	Co	Ni
10	90	8.5	91.6	–	–	–	–
20	80	17.7	82.3	19.8	80.2	17.8	82.2
30	70	25.1	74.9	24.9	75.1	24.3	75.7
40	60	42.3	57.7	43.1	56.9	42.6	57.4
50	50	46.7	53.3	45.5	54.5	47.2	52.7
60	40	57.0	43.0	56.5	43.5	57.3	42.7
70	30	68.4	31.6	69.8	30.2	66.9	33.1
80	20	76.2	23.8	75.1	24.9	76.4	23.6
90	10	87.1	12.9	86.4	13.6	88.0	12.0

Table 1 presents data that allow a comparison of the composition of the bulk alloys and alloy films. For the films, a fairly good coincidence of the calculated and determined chemical composition by X-ray microanalysis is also observed. It should be noted, however, that when studying films, the intensity of X-ray radiation is much (10-20 times) lower than for bulk materials, due to the small mass of the substance in the studied area. It is obvious that under such conditions, significant statistical deviations of the true concentrations of components are possible in comparison with the data obtained using the computer software for the microanalyzer. In addition, the computer program attached to the microanalyzer, when obtaining the final result, takes into account corrections caused by a number of effects, such as the absorption of X-ray radiation in the thickness of the sample, the value of the atomic number of the element and secondary fluorescence. These effects occur for bulk samples, but in the case of our films they can be neglected due to the relatively small number of atoms in the thickness of the film in the area from which the X-ray generation occurs. As a result, when calculating the composition of a film alloy, it is more correct to use the ratio of the intensities of characteristic radiation lines measured using EDS, obtained from film samples without taking into account the corrections due to the above effects (without processing the obtained results using software).

These considerations are well confirmed by the data given in Table 1. Comparing the results of microanalysis of bulk samples and films, we see that the calculation of

the composition of films using the microanalyzer software gives larger deviations of the composition of films from the composition of bulk samples. Due to minor differences in the wavelengths of the characteristic lines of the K α series for Fe, Co and Ni, the use of the microanalyzer software in spectrum analysis led to the detection of CoNi as a possible element of Fe with a small concentration in the composition of the samples. However, the intensity of the characteristic X-ray radiation lines of Fe is practically at the background level and is significantly lower than the intensity of the characteristic radiation of the main elements (Co and Ni). In the spectra of film samples, a number of characteristic X-ray radiation lines of the elements included in the composition of the glass substrate are also observed (part of the lines in the left half of the spectra, Fig. 6). When calculating the composition of the samples, they were not taken into account and the data for the films given in Table 1 were calculated taking into account these remarks. Summarizing these considerations, it can be stated that the proposed technology for obtaining CoNi film alloys (using samples of known composition) allows obtaining films of these alloys with a predetermined content of components.

3.2 FeNi Alloy Films

To obtain FeNi alloy films, we used an alloy known as Permalloy 50N. Fig. 8 and Table 2 show the results of the study of the composition of the bulk FeNi alloy and FeNi alloy films of different thicknesses. According to microanalysis, the starting material contains approximately 50-52 wt. % Fe and 48-50 wt. % Ni, which, within the analysis error, corresponds to the literature data on the composition of this alloy (49.5-50.0 wt. % Ni, impurities (Si, Mn) < 1 wt. %, the rest Fe [9]).

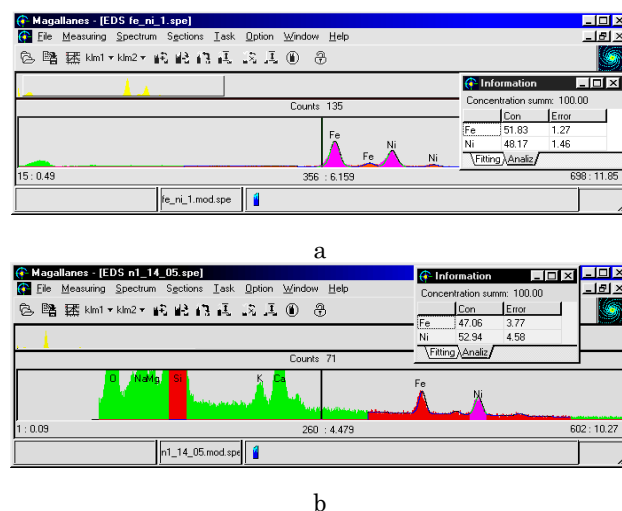


Fig. 8 – Characteristic X-ray spectrum from the bulk alloy 50H (a) and the film (b) with a thickness $d = 140$ nm

The characteristic X-ray lines in the left part of the spectrum from the alloy films (Fig. 8 b), as in the case of CoNi alloy films, correspond to the material of the glass substrate. Processing of spectra using computer software of the microanalyzer shows that the composition of the obtained films is somewhat different from the composition of the original alloy (approximately 44-47 at. % Fe and 53-56 at. % Ni).

Table 2 – Results of the study of the elemental composition of bulk and film FeNi alloys

	Calculation using software taking into account corrections				Calculation without taking into account corrections			
	C _{Fe} , at. %	C _{Ni} , at. %	c _{Fe} , wt. %	c _{Ni} , wt. %	C _{Fe} , at. %	C _{Ni} , at. %	c _{Fe} , wt. %	c _{Ni} , wt. %
Bulk FeNi alloy (50N)	51.8	48.2	50.6	49.4	—	—	—	—
	53.4	46.6	52.2	47.8				
Thickness film FeNi alloy, nm								
47	43.9	56.1	42.7	57.3	51.3	48.7	50.1	49.9
100	46.9	53.1	45.7	54.3	50.4	49.6	49.2	50.8
110	47.7	52.3	46.5	53.5	53.7	46.3	52.5	47.5
120	47.1	52.9	45.9	54.1	53.8	46.2	52.7	47.3
140	47.1	52.9	45.9	54.1	53.8	46.2	52.7	47.3

However, it should be noted that the error in determining the composition of film samples (especially with a small thickness) is greater than for a bulk sample, as in the case of CoNi alloy films (a small amount of substance in the film material and, as a result, the deviation of real spectra from the model ones obtained by mathematical processing). On the other hand, since the energy of photons of the characteristic radiation of Ni is greater than that of Fe, secondary fluorescence may occur in the bulk material. In this case, the intensity of the Ni line decreases, and the intensity of the Fe line, on the con-

trary, increases. The computer program of the mathematical software of the microanalyzer provides for the introduction of a correction for fluorescence when determining the concentration. However, as mentioned earlier, in film samples this effect can be neglected, as a result of which the program gives inflated values of the Ni content. Table 2 also shows the values of the Fe concentration obtained without taking into account the corrections, which are in the range of 50-53 wt. %, which better corresponds to the composition of the starting material. With increasing film thickness, the iron content increases slightly (according to the results of microanalysis), which is explained by the enrichment of the condensed film with iron due to differences in the values of the vapor pressure and evaporation rates of the components.

4. CONCLUSIONS

1. The results of the study of the elemental composition of alloy films using X-ray microanalysis methods indicate the high purity of the films.

2. A study of the chemical composition of CoNi and FeNi alloy films showed that the content of elements in the film generally corresponds to their content in the bulk material.

3. The proposed method for obtaining CoNi alloy films by evaporation of samples of known composition allows obtaining films of these alloys with a predetermined content of components.

REFERENCES

- V.K. Soni, S. Sanyal, S.K. Sinha, *Vacuum* **174**, 109173 (2020).
- L.V. Odnodvoretz, I.Y. Protsenko, O.P. Tkach, Y.M. Shabelnyk, N.I. Shumakova, *J. Nano-Electron. Phys.* **9** No 2, 02021 (2017).
- Y.S. Berezhnyak, M. Opielak, L.V. Odnodvoretz, D. Poduremne, I.Y. Protsenko, Yu.M. Shabelnyk, *J. Nano-Electron. Phys.* **11** No 2, 02026 (2019).
- V.B. Loboda, V.M. Kolomiets, S.M. Khursenko, Yu.O. Shkurdoda, *J. Nano-Electron. Phys.* **6** No 1, 04032 (2014).
- O.V. Bezdidko, S.A. Nepijko, Y.O. Shkurdoda, Yu.M. Shabelnyk, *J. Nano-Electron. Phys.* **13** No 3, 03042 (2021).
- A.D. Pogrebnyak, A.G. Lebed, Yu.F. Ivanov, *Vacuum* **63** No 4, 483 (2001).
- A.D. Pogrebnyak, I.V. Yakushchenko, G. Abadias, P. Chartier, O.V. Bondar, V.M. Beresnev, Y. Takeda, O.V. Sobol', K. Oyoshi, A.A. Andreyev, B.A. Mukushev, *J. Superhard Mater.* **35** No 6, 356 (2013).
- H. Frey, H.R. Khan, *Handbook of Thin-Film Technology* (Berlin: Springer-Verlag: 2015).
- H. Okamoto, M.E. Schlesinger, E.M. Mueller, *Alloy Phase Diagrams* (Novelty: ASM International: 2016).
- K.L. Kapoor, *A Textbook of Physical Chemistry: 3rd (3 volumes) Edition* (Gurgaon: MACMILLAN: 2012).
- W. Benenson, J.W. Harris, H. Stocker, H. Lutz, *Handbook of Physics* (New York: Springer-Verlag: 2002).
- V.B. Loboda, V.M. Zubko, S.M. Khursenko, V.O. Kravchenko, A.V. Chepizhnyi, *J. Nano-Electron. Phys.* **15** No 5, 05014 (2023).
- J.I. Goldstein, D.E. Newbury, P. Echlin, D.C. Joy, C.E. Lyman, E. Lifshin, J.R. Michael, *Scanning Electron Microscopy and X-ray Microanalysis* (New York: Springer Science + Business Media: 2003).

Дослідження елементного складу тонких нанокристалічних плівок сплавів CoNi та FeNi методом рентгеноспектрального мікроаналізу

В.Б. Лобода, С.М. Хурсенко, В.М. Зубко, В.О. Кравченко, А.В. Чепіжний

Сумський національний аграрний університет, 40021 Суми, Україна

У статті наведено результати дослідження елементного складу нанокристалічних плівок сплавів CoNi та FeNi методом рентгенівського мікроаналізу (рентгенівський мікроаналізатор на базі спектрометра з дисперсією за енергією, що входить до складу растрового електронного мікроскопа PEM-103-01). Плівки сплавів завтовшки 10-200 нм були отримані конденсацією випарених вихідних масивних бінарних сплавів CoNi та FeNi у вакуумі 10⁻⁴ Па. Сплави CoNi випаровувалися електронно-променевим способом за допомогою електронної діодної гармати зі швидкістю конденсації 0,5-1,5 нм/с. Чистота ви-

хідних металів Co та Ni становила не менше 99,9 %. Концентрації компонент плівок сплаву CoNi змінювалися в широкому діапазоні. Плівки сплаву FeNi були отримані в результаті випаровування технічного сплаву пермалою 50Н. Характеристичний рентгенівський спектр речовини плівки збуджувався при скануванні електронним пучком ділянки плівки розмірами 300×300 мкм; для товстіших плівок розмір ділянки сканування становив 1×1 мкм. Як еталони при проведенні кількісних вимірювань елементного складу плівок сплавів певної товщини використовувалися тонкі плівки Ni такої ж товщини. Результати рентгенівського мікроаналізу свідчать про високу чистоту плівок. Зіставлення результатів вимірювань рентгенівським мікроаналізом концентрацій вихідних сплавів та отриманих плівок показало їх збіг у межах похибки аналізу.

Ключові слова: Рентгеноспектральний мікроаналіз, Хімічний склад, Тонкі плівки, Нанокристалічні плівки, Сплави.